Volume 1 | Number 1 | Jan 2013 | Pages 1–100

Journal of
Materials Chemistry B

Materials for biology and medicine
www.rsc.org/materialsB

ROYAL SOCIETY OF CHEMISTRY

ROYAL SOCIETY OF CHEMISTRY

www.rsc.org/materialsB

Journal of Materials Chemistry B

COMMUNICATION

Metals & Polymers in the Mix: Fine-Tuning the Mechanical Properties & Color of Self-healing Mussel-inspired Hydrogels

Marie Krogsgaard, Michael Ryan Hansen and Henrik Birkedal[*]

**Reversible sacrificial bonds play a crucial role in various biological materials where they serve as load-bearing bonds, facilitating extensibility and/or impart self-healing properties to the biological materials. Recently, the coordination bonds found in blue mussel byssal threads have been mimicked in the design of self-healing hydrogels. Herein we show how the mechanical moduli of mussel-inspired hydrogels based on DOPA-polyallylamine (DOPA-PAA) can be straight-forwardly adjusted by systematically varying the coordinating metal from Al^{III}, Ga^{III} to In^{III}. These gels are transparent and only slightly tanned opposite to the black hydrogels obtained using Fe^{III}. Additionally, dark Fe^{III}:DOPA-chitosan gels were synthesized and showed remarkably high storage modulus. The strongest hydrogels were formed around pH 8, which is closer to physiological pH than what was observed in the Fe^{III}:DOPA-PAA system ($pH_{max} \sim 9.5$). This finding supports the hypothesis that the maximum in the storage modulus distribution can be adjusted to match a given application by selecting the cationic polymer based on its pK_a value.**

Nature has developed many different materials with unique and desirable properties[1]. In the past couple of decades the blue mussel has attracted great attention due to its ability to form strong under-water bonds to a wide range of surfaces[2]. The secret behind these amazing sticking powers has been shown to be high amounts of the amino acid DOPA[3]. Furthermore, the mussel incorporates Fe^{III} ions in a DOPA rich byssus coating[4], which imbues it with strength and self-healing properties through the formation of strong, yet reversible DOPA-Fe^{III} coordination bonds[4b]. The number of DOPAs bound per Fe^{III} is highly pH-dependent[5] and consequently, the mussel glue cures in a pH-dependent manner (Scheme 1a). The chemistry of the byssus has been used as inspiration in several biomimetic materials[2, 6]. Of particular relevance to the present study, the metal coordination capability has been mimicked in the formation of self-healing pH-responsive hydrogels of catechol functionalized polymers cross-linked by iron ions[6a, 7]. Similarly,

Nereis worm jaws are formed by histidine rich proteins reinforced by coordination bonds with zinc ions[8]. This has led to the formation of worm jaw inspired materials[9] as has similar histidine/metal motifs in mussel byssi[10].
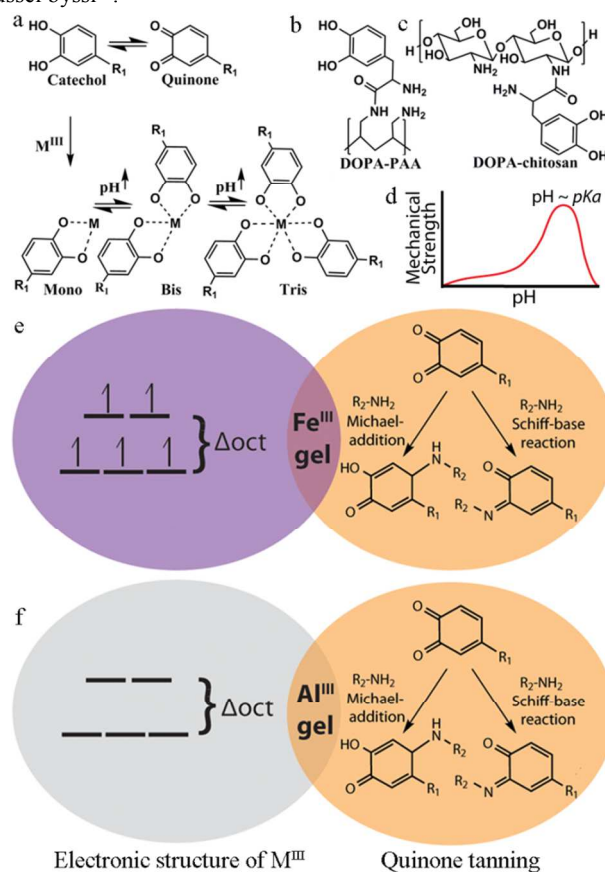
Scheme 1. (a) Chemical structure of DOPA's catechol and quinone form, including the catchol's ability to react with hard metal ions. M^{III}. Chemical structure of (b) DOPA-PAA ($pK_a \sim 9.5$) and (c) DOPA-chitosan ($pK_a \sim 6.7$). (d) Schematic of the characteristic peak-shaped storage modulus distribution expected using amine containing polymers. (e) and (f) illustrate the two major

contributions to the gel color in Fe^{III} and $Al^{III}/Ga^{III}/In^{III}$ based gels, respectively. The intersections depict the resulting color of the gels.

The mussel adhesive proteins are basic due to a high lysine content[1c, 2, 11]. Recently, we made biomimetic polymers based on polyallylamine on which DOPA was grafted to emulate the cationic nature of the catechol containing mussel proteins[7b] (DOPA-PAA, Scheme 1b). The DOPA-PAA polymer was cross-linked by Fe^{III}, resulting in pitch black hydrogels that displayed a peak-shaped modulus distribution as a function of pH with a maximum around the polymer's pK_a value ($pH_{max} \sim 9.5 \sim pK_a$). A schematic illustration of the characteristic modulus distribution is depicted in Scheme 1d. However, our previous work left two questions unanswered, which are the focus of the present paper. The first question is whether the multi-pH-responsive design allows for the maximum in the modulus distribution to be adjusted to a given pH value determined by the cationic polymer's pK_a value.[7b] To investigate this, DOPA-chitosan was synthesized (Scheme 1c, See also supplementary materials, ESI). DOPA-chitosan has a lower pK_a value than DOPA-PAA (6.7 vs. 9.5, ESI), making it a good candidate for addressing this question as it is expected to result in a shift in the modulus distribution towards physiological pH. Additionally, chitosan has the advantage that it is a relatively inexpensive natural polymer, which in general is considered to be safe for use in biological settings due to its biodegradable[12] and biocompatible[13] nature. Accordingly, DOPA-chitosan and catechol/chitosan based systems have been widely studied in the literature[14]. The second question arising from our work on Fe^{III}:DOPA-PAA hydrogels is whether the color and modulus can be adjusted by systematically varying the employed metal? To answer this question, DOPA-PAA was cross-linked using the group 13 elements (group IIIA/IIIB); Al^{III}, Ga^{III} and In^{III} and the mechanical properties of the formed gels were assessed by rheology.

Addressing the first question, Fe^{III}:DOPA-chitosan hydrogels were created in accordance with our previously published recipe (ESI)[7b]. In brief, DOPA-chitosan with a grafting density of ~3.3% was dissolved and mixed with Fe^{III} ions at pH 1. A pitch black gel was formed by increasing the pH to ≥ 6 using NaOH (catechol:Fe^{III} ratio of 3:1, Figure S1). The pH-dependent assembly of the hydrogels was monitored using UV/VIS absorbance spectroscopy (ESI) as the Fe^{III}:catechol coordination bonds display characteristic absorptions in the visible range[5] (Figure 1a). As the pH is increased from acidic to alkaline, the color of the solution changes from faint green, to blue to red, which can be assigned to the presences of mono-, bis- and tris-species, respectively (See inserts in Figure 1a). The colors are in line with what previously have been observed for similar systems[7a, 7b, 15]. The mechanical properties of the hydrogels were assessed by performing frequency sweeps using rheology (Figure S2a,b, ESI). The material was found to be in a liquid state at pH 4 (Storage modulus, G' < loss modulus, G'') and then as the pH is increased from acidic to intermediate values (pH 8), the elastic response of the material starts to dominate ($G' > G''$) owing to the change in bond stoichiometry (Scheme 1a). As the pH is further increased to alkaline values, the viscous response of the material takes over ($G' < G''$) and the material becomes more liquid-like again, indicating that the

hydrogel system displays a peak in the pH dependence of the gel modulus just like the previously published Fe^{III}:DOPA-PAA system (Scheme 1d)[7b]. To clarify this point further, the obtained storage modulus G', (used as a measure of the gel mechanical stiffness) was plotted as a function of pH for an angular frequency of 25 s^{-1} (Figure 1b). The modulus distribution displays a distinct peak at pH 8 with a remarkably high modulus (30 kPa). The result supports the hypothesis that the multi-pH responsive design leads to a hydrogel system with a peak-shaped modulus distribution (Scheme 1d and Figure 1b) and that the polymer mechanics can be shifted towards a preferred pH value by careful selection of the cationic polymer.
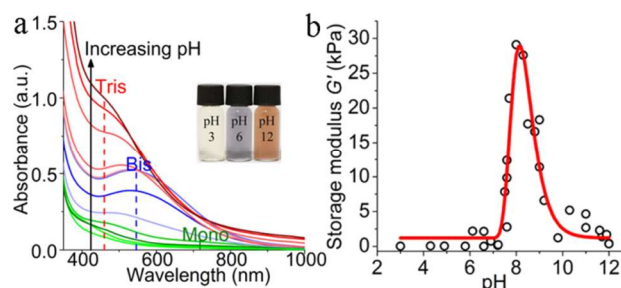

Fig. 1(a) Absorption profiles of Fe^{III}:DOPA-chitosan solutions at pH 1-12. The black arrow points in the direction of increasing pH. The characteristic mono- (~720 nm), bis- (~547 nm) and tris- (~460 nm) peaks are highlighted. The inserts show the color of the solution at pH 3, 6 and 12, where the mono-, bis- and tris- species prevail. (b) Storage modulus (G') plotted as a function of pH (black) at an angular frequency of 25 s^{-1}. The red line serves as a guide to the eye.

As shown above, iron cross-linked hydrogels are strongly colored[2a, b]. For many applications uncolored and/or transparent materials are preferred due to cosmetic or practical reasons. The color of metal-cross-linked catechol-polymer systems is predominantly determined by two factors: *1)* the electronic structure of the metal[16] and *2)* the degree of catechol oxidation and quinone tanning; both are schematically depicted in Scheme 1e and f. The electronic structure matters as transition metals with partially filled d-orbitals such as Fe^{III}, form strongly colored gels (Scheme 1e) with major contributions from d-d transitions[16]. On the contrary, metal ions with empty or filled d-shells (or f-shells) form slightly tanned gels as the only source of color comes from oxidation processes that are catalysed by high pH (Scheme 1f)[17]. Here, catechols are oxidized to quinones (Scheme 1a). The formed quinones are susceptible towards nucleophilic attacks and create amongst others covalent bonds to amines on the polymer backbone, resulting in colored products (quinone tanning, Scheme 1e and f)[18]. Accordingly, the color derived from d-d transitions can be bypassed by using main group metals such as $Al^{III}/Ga^{III}/In^{III}$, which do not have partially filled d-orbitals. In addition, it has been speculated that Fe^{III} can catalyse catechol oxidation due to its available Fe^{II} state[7e, 19]. This potential metal-triggered oxidation can thus be avoided by using these alternative metals with only one available oxidation state.

In the present work, transparent and slightly orange hydrogels were formed by cross-linking DOPA-PAA (Scheme 1b) using

Al[III]/Ga[III]/In[III]. In addition to the lighter color, the modulus of the gels is also dependent on the interaction between polymer and metal (e.g. through the hardness of the metal ion according to the hard/soft acid/base principle). The group 13 metals enable a systematic study of how the hardness of the cation affects the mechanical properties of the hydrogels. When moving down the group, the hardness falls and this is expected to lead to lower binding strengths to the hard catechol ligands. Al[III] cross-linked catechol-PEG hydrogels have previously been investigated[7d, 20] but no systematic variation of cation has so far been reported.

The M[III]:DOPA-PAA hydrogels were created following our previously published recipe (ESI)[7b]. Upon base addition, the materials changed from colorless liquids to orange self-healing hydrogels as seen in Figure 2a. The self-healing ability of the gels was qualitatively tested by cleaving a freshly formed gel, bringing the pieces into contact, and monitoring the recovery of the gel structure (Figure 2a). After 2-7 min, the external structure of the hydrogel blobs was fully recovered, confirming the reversible nature of the coordination bond and the gel's viscoelastic behaviour. The self-healing properties were quantitatively investigated using rheology (ESI). Here, M[III] based gels (pH 6, 9 and 12) were strained until failure after which the recovery was monitored. Regardless of pH and metal system, the hydrogels were found to fully recover to their original modulus. In Figure 2b the data for Al[III] and Fe[III] (pH 8) gels are compared. While both display rapid self-healing capabilities, the Al[III] gel is almost a factor of two less strong than the Fe[III] gel, confirming that the gel modulus depends on the catechol affinity of the metal.
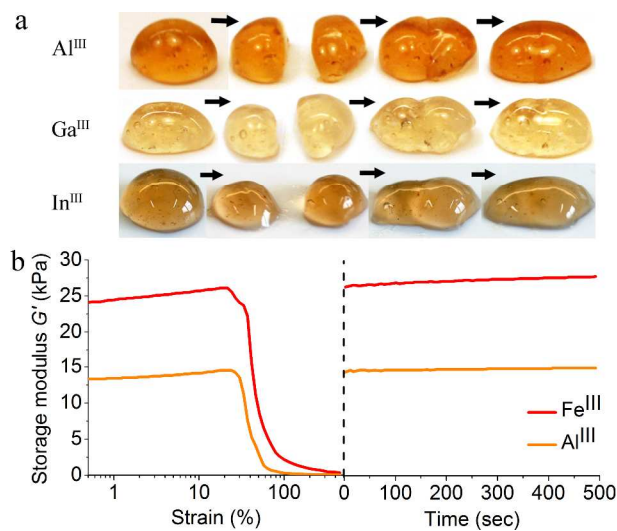

Fig. 2 (a) Qualitative tests of the self-healing properties of Al[III], Ga[III] and In[III] gels. (b) Quantitative tests of the self-healing properties of Al[III] and Fe[III] gels.

When using metals such as Al[III]/Ga[III]/In[III] without electronic transitions in the visible range, UV-VIS spectroscopy cannot be straightforwardly used to probe coordination states as done in the Fe[III]:DOPA-chitosan system (Figure 1a); indeed the lack of coordination related absorption bands results from the absence of partially filled *d*-orbitals (Scheme 1e and f), however, it is not a sign of lack of coordination as suggested by others[20]. To establish the evolution of metal coordination with pH, other experimental techniques are needed. Herein, we used extended X-ray absorption fine structure (EXAFS) on Ga[III] based gels to probe the local metal coordination environment at different pH values. The measurements were recorded in fluorescence mode at the I811 MaxLAB beam line (Lund, Sweden, ESI). The normalized absorption curves and corresponding radial distribution functions are shown in Figure 3 together with a schematic highlighting the first and second coordination shells of the different bond stoichiometries.
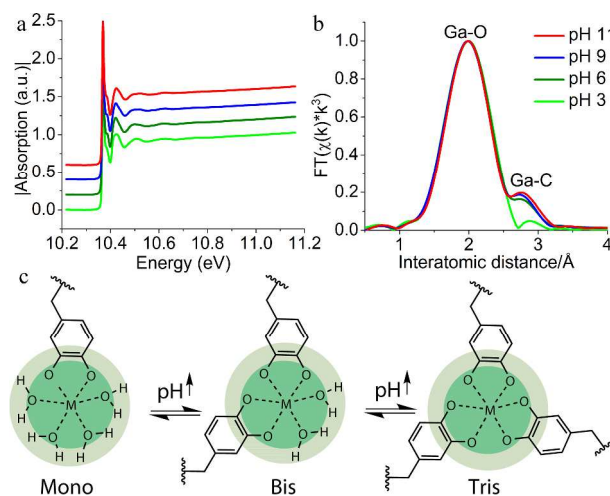

Fig. 3 (a) Normalized and background subtracted Ga K-edge EXAFS curves for pH 3, 6, 9 and 11 gels. The curves have been shifted along the y-axis and the legend is shown in (b). (b) Radial distribution functions. (c) Schematic drawing of the different M[III]:catechol bond stoichiometries, highlighting the first and second coordination shells.

The first coordination shell contains six oxygen atoms located on a combination of catechol moieties and/or water molecules depending on bond stoichiometry (Figure 3c). The oxygen atoms have identical scattering intensities and accordingly, the second coordination sphere has to be addressed to investigate how the bond stoichiometry evolves with pH. The second sphere appears as a shoulder to the right of the first shell in the radial distribution functions. The area of the second shell increases with pH in agreement with the increasing number of carbon atoms present in this coordination sphere (Figure 3c). This finding is consistent with the gels becoming increasingly cross-linked as the pH is increased. Further insights into the gelation behaviour were obtained by ^{1}H NMR on solutions of Al[III]:DOPA-PAA as summarized in Figure S4. With increasing pH the ^{1}H resonances broaden due to restricted molecular mobility of the DOPA-PAA polymer chains[21]. These observations are in agreement with hydrogel formation and the materials design (Scheme 1a). Moreover, a closer inspection of the sp^2 region (5.5 – 8 ppm, Figure S4b) reveals ^{1}H peak shifts, which may support the fact that the catechols become oxidized as the pH is increased.

The mechanical properties of the Al[III]/Ga[III]/In[III] based hydrogels were assessed by performing frequency sweeps at various pH values using rheology (see ESI for details and Figure S2c and d for

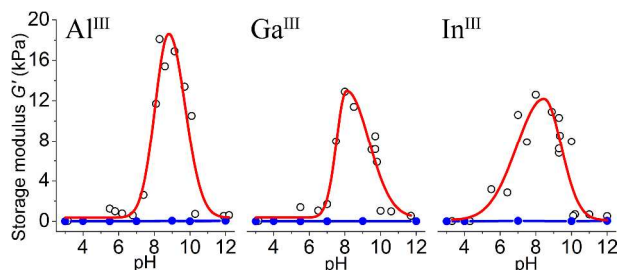frequency sweeps performed on Al^{III} based materials). Figure 4 shows the resulting modulus distributions.

Fig. 4 Storage modulus (G') plotted as a function of pH for the different metal systems (Al^{III}, Ga^{III} and In^{III}) at an angular frequency of 25 s^{-1}. The red line serves as a guide to the eye. The polyallyamine:M^{III} references are shown in blue.

As expected, the hydrogels display peak-shaped storage modules distributions (Scheme 1d) with maxima close to, but still slightly lower than the pK_a value of PAA ($pK_a \sim 9.5$). This suggests that the position of the distribution is not solely controlled by the polymer's pK_a but also by the nature of the coordinating metal. When comparing the determined maximum moduli, it is found to decrease from Al^{III} (18.5 kPa, pH 8.8) to Ga^{III} (13 kPa, pH 8.1) to In^{III} (12 kPa, pH 8.5). This is in line with the decreasing metal hardness observed when moving down the group 13, confirming the hypothesis that the mechanical properties of the gels can be fine-tuned by systematically varying the employed metal. The storage moduli are substantially higher in the cationic systems (DOPA-chitosan and DOPA-PAA) than in the corresponding neutral systems by Holten-Andersen et al[7a]. This difference is largely due to difference in the polymer concentration that is higher in the present polycationic systems. Additionally the DOPA concentration is higher in the present g-DOPA-PAA materials while it is similar for g-DOPA-chitosan. These factors lead to a higher degree of polymer cross-linking and entanglement resulting in higher storage moduli. Furthermore, chitosan has a tendency to self-aggregate, which may contribute further to the high storage moduli obtained in the DOPA-chitosan system (Figure 1b)[22].

The Al^{III}/Ga^{III}/In^{III} based hydrogels were found to be transparent and slightly tanned (Figure 2a). At high pH the gels developed a more pronounced orange color, which is assigned to the pH-dependent catechol oxidation followed by quinone tanning (Scheme 1a, e and f). The oxidation process was examined by performing UV-VIS absorption measurements on solutions of M^{III}:DOPA-PAA (ESI). The absorption profiles associated with the different metal systems displayed no substantial difference and accordingly, only the absorption data associated with Al^{III} are presented (Figure 5). The samples show strong absorptions in the ultraviolet range, which can be assigned to the k- and b-band of the catechol and to various electronic transitions. As the pH is increased, absorption in the visible range (>390 nm) appears which can be explained by the formation of irreversible products from quinone tanning. This result was further supported by the fact that the band did not disappear when lowering the pH to 1 after having reached pH 12, confirming

that the formed products are irreversible (Figure 5a). The absorption measured at pH 12 in air was compared with that of a similar sample prepared under nitrogen (Figure 5b). Whereas the sample prepared in air absorbed visible light and was orange, the sample prepared under nitrogen was colorless and showed no absorption in the visible range, confirming that the orange color originates from oxidation processes (Scheme 1e, f). To further investigate the pH-dependent balance between covalent and coordination bonds, gels with three different pH values (pH 6, 9, and 12) were immersed in solutions of EDTA (ESI). The gels were found to become decreasingly soluble in EDTA with increasing pH (Figure S5). This supports the interpretation, that the pH-catalyzed oxidation plays a role in the formation of the gels.
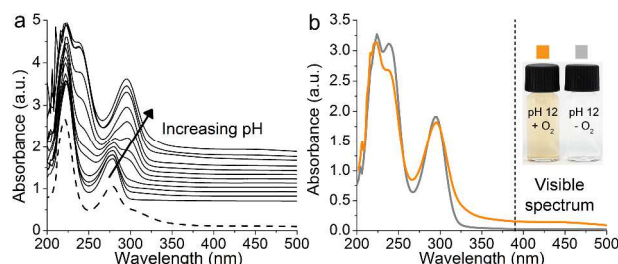

Fig. 5 (a) Absorption profiles at different pH values of solutions of Al^{III}:DOPA-PAA. The arrow points in the direction of increasing pH. The dashed curve shows the absorption at pH 1 after having reached pH 12. The absorption profiles have been shifted along the y-axis. (b) Comparison of the absorption profiles measured at pH 12 in air and under N_2. The inserts show the color of the samples.

Accordingly, unwanted auto-oxidation, coloring and covalent bond formation can be prevented by inhibiting oxidation via the removal of molecular oxygen as done above using a nitrogen atmosphere. In more practical terms, we prevented oxidation by the addition of an anti-oxidant such as ascorbic acid (Figure S3). Nevertheless, in concentrated gels, the anti-oxidizing capability of ascorbic acid is not strong enough to fully avoid oxidation, resulting in tanned gels. The use of antioxidants to control oxidation kinetics may also play a role in mussel byssi. Indeed, the thiol-rich mussel foot protein 6 (mfp-6) found in the adhesive plaque has been shown to be able to rescue the adhesive capabilities of the DOPA-rich mfp-3, indicating that antioxidants are important in mussel adhesion[23]. Our present work using the non-byssus relevant antioxidant ascorbic acid lends further support to this notion and provides an impetus for further work on oxidation control in DOPA based self-healing gels.

Conclusions

In this work, Fe^{III}:DOPA-chitosan hydrogels were formed, which showed remarkable storage moduli of up to ~30 kPa. As hypothesized, the maximum storage modulus was shifted towards physiological pH by using DOPA-chitosan instead of DOPA-PAA. This result indicates that the mechanical properties can be adjusted by selecting the polymer based on its pK_a value. In the second part of this work, it was shown that the color and the mechanics of the gels can be fine-tuned systematically by varying the coordinating metal. Moreover, the experiments involving antioxidants suggest that a

proper antioxidant will be able to fully prevent auto-oxidation from occurring in the gels.

Acknowledgements

Notes and references

iNANO & Department of Chemistry, Aarhus University, Gustav Wieds Vej 14, DK-8000 Aarhus, Denmark. Corresponding author: HB. Email: hbirkedal@chem.au.dk.

1. (a) J. W. C. Dunlop and P. Fratzl, *Annu. Rev. Mater. Res.*, 2010, **40**, 1-24; (b) M. A. Meyers, P.-Y. Chen, A. Y.-M. Lin and Y. Seki, *Prog. Mater. Sci.*, 2008, **53**, 1-206; (c) D. J. Rubin, A. Miserez and J. H. Waite, *Adv. Insect Phys.*, 2010, **38**, 75-133.

2. B. P. Lee, P. B. Messersmith, J. N. Israelachvili and J. H. Waite, *Annu. Rev. Mater. Res.*, 2011, **41**, 99-132.

3. J. H. Waite and X. Qin, *Biochemistry*, 2001, **40**, 2887-2893.

4. (a) M. J. Harrington, A. Masic, N. Holten-Andersen, J. H. Waite and P. Fratzl, *Science*, 2010, **328**, 216-220; (b) N. Holten-Andersen, G. E. Fantner, S. Hohlbauch, J. H. Waite and F. W. Zok, *Nat. Mater.*, 2007, **6**, 669-672; (c) N. Holten-Andersen, T. E. Mates, M. S. Toprak, G. D. Stucky, F. W. Zok and J. H. Waite, *Langmuir*, 2008, **25**, 3323-3326.

5. S. W. Taylor, D. B. Chase, M. H. Emptage, M. J. Nelson and J. H. Waite, *Inorg. Chem.*, 1996, **35**, 7572-7577.

6. (a) Z. Shafiq, J. Cui, L. Pastor-Pérez, V. San Miguel, R. A. Gropeanu, C. Serrano and A. del Campo, *Angew. Chem. Int. Ed.*, 2012, **51**, 4332-4335; (b) C. E. Brubaker and P. B. Messersmith, *Biomacromolecules*, 2011, **12**, 4326-4334; (c) H. Lee, B. P. Lee and P. B. Messersmith, *Nature*, 2007, **448**, 338-341; (d) B. P. Lee, J. L. Dalsin and P. B. Messersmith, *Biomacromolecules*, 2002, **3**, 1038-1047; (e) H. Lee, S. M. Dellatore, W. M. Miller and P. B. Messersmith, *Science*, 2007, **318**, 426-430; (f) M. Vatankhah-Varnoosfaderani, S. Hashmi, A. GhavamiNejad and F. J. Stadler, *Polym. Chem.*, 2014, **5**, 512-523; (g) B. J. Sparks, E. F. T. Hoff, L. P. Hayes and D. L. Patton, *Chem. Mater.*, 2012, **24**, 3633-3642; (h) L. Garcia-Fernandez, J. X. Cui, C. Serrano, Z. Shafiq, R. A. Gropeanu, V. San Miguel, J. I. Ramos, M. Wang, G. K. Auernhammer, S. Ritz, A. A. Golriz, R. Berger, M. Wagner and A. del Campo, *Adv. Mater.*, 2013, **25**, 529-533; (i) Z. Hongbo, H. Dong Soo, J. N. Israelachvili and J. H. Waite, *PNAS*, 2010, **107**, 12850-12853; (j) G. Fichman, L. Adler-Abramovich, S. Manohar, I. Mironi-Harpaz, T. Guterman, D. Seliktar, P. B. Messersmith and E. Gazit, *ACS Nano*, 2014, **8**, 7220-7228; (k) C. R. Matos-Pérez, J. D. White and J. J. Wilker, *J. Am. Chem. Soc.*, 2012, **134**, 9498-9505; (l) C. R. Matos-Pérez and J. J. Wilker, *Macromolecules*, 2012, **45**, 6634-6639; (m) E. Faure, C. Falentin-Daudre, T. S. Lanero, C. Vreuls, G. Zocchi, C. Van De Weerdt, J. Martial, C. Jérôme, A. S. Duwez and C. Detrembleur, *Adv. Func. Mater.*, 2012, **22**, 5271-5282; (n) H. Lee, N. F. Scherer and P. B. Messersmith, *PNAS*, 2006, **103**, 12999-13003; (o) J. Sedo, J. Saiz-Poseu, F. Busque and D. Ruiz-Molina, *Advanced Materials*, 2013, **25**, 653-701.

7. (a) N. Holten-Andersen, M. J. Harrington, H. Birkedal, B. P. Lee, P. B. Messersmith, K. Y. C. Lee and J. H. Waite, *PNAS*, 2011, **108**, 2651-2655; (b) M. Krogsgaard, M. A. Behrens, J. S. Pedersen and H. Birkedal, *Biomacromolecules*, 2013, **14**, 297-301; (c) M. Krogsgaard, A. Andersen and H. Birkedal, *Chem. Comm.*, 2014, **50**, 13278-13281; (d) M. S. Menyo, C. J. Hawker and J. H. Waite, *Soft Matter*, 2013, **9**, 10314-10323; (e) D. E. Fullenkamp, D. G. Barrett, D. R. Miller, J. W. Kurutz and P. Messersmith, *RSC Advances*, 2014, **4**, 25127-25134; (f) M. J. Sever, J. T. Weisser, J. Monahan, S. Srinivasan and J. J. Wilker, *Angew. Chem. Int. Ed.*, 2004, **43**, 448-450; (g) B. J. Kim, D. X. Oh, S. Kim, J. H. Seo, D. S. Hwang, A. Masic, D. K. Han and H. J. Cha, *Biomacromolecules*, 2014, **15**, 1579-1585.

8. (a) H. Birkedal, R. K. Khan, N. Slack, C. Broomell, H. C. Lichtenegger, F. Zok, G. D. Stucky and J. H. Waite, *ChemBioChem*, 2006, **7**, 1392-1399; (b) H. C. Lichtenegger, T. Schoberl, J. T. Ruokolainen, J. O. Cross, S. M. Heald, H. Birkedal, J. H. Waite and G. D. Stucky, *PNAS*, 2003, **100**, 9144-9149; (c) H. C. Lichtenegger, H. Birkedal and J. H. Waite, *Metal Ions in Life Sciences*, 2008, 295-325.

9. A. Srivastava, N. Holten-Andersen, G. D. Stucky and J. H. Waite, *Biomacromolecules*, 2008, **9**, 2873-2880.

10. D. E. Fullenkamp, L. He, D. G. Barrett, W. R. Burghardt and P. B. Messersmith, *Macromolecules*, 2013, **46**, 1167-1174.

11. J. H. Waite and X.-X. Qin, *Biochemistry*, 2001, **40**, 2887-2893.

12. (a) K. Tomihata and Y. Ikada, *Biomaterials*, 1997, **18**, 567-575; (b) H. Yamamoto and M. Amaike, *Macromolecules*, 1997, **30**, 3936-3937.

13. S. W. Richardson, H. J. Kolbe and R. Duncan, *Int. J. Pharmaceutics*, 1999, **178**, 231-243.

14. (a) J. H. Ryu, Y. Lee, W. H. Kong, T. G. Kim, T. G. Park and H. Lee, *Biomacromolecules*, 2011, **12**, 2653-2659; (b) Y. C. Zhang, Y. Thomas, E. Kim and G. F. Payne, *J. Phys. Chem. B*, 2012, **116**, 1579-1585; (c) D. X. Oh and D. S. Hwang, *Biotechnol. Prog.*, 2013, **29**, 505-512.

15. H. Ejima, J. J. Richardson, K. Liang, J. P. Best, M. P. van Koeverden, G. K. Such, J. Cui and F. Caruso, *Science*, 2013, **341**, 154-157.

16. C. J. Jones, *d- and f- Block Chemistry*, 2001.

17. J. H. Waite, *Comp. Biochem. physiol.*, 1990, **97B**, 19-29.

18. T. J. Deming, *Cur. Op. Chem. Biol.*, 1999, **3**, 100-105.

19. H. G. Jang, D. D. Cox and L. Que, *J. Am. Chem. Soc.*, 1991, **113**, 9200-9204.

20. N. Holten-Andersen, A. Jaishankar, M. J. Harrington, D. E. Fullenkamp, G. DiMarco, L. He, G. H. McKinley, P. B. Messersmith and K. Y. C. Lee, *J. Mater. Chem. B*, 2014, **2**, 2467-2472.

21. (a) K. Schmidt-Rohr and H. W. Spiess, *Multidimensional solid-state NMR and Polymers*, 1994; (b) S. Inal, L. Chiappisi, J. D. Kölsch, M. Kraft, M.-S. Appavou, U. Scherf, M. Wagner, M. R. Hansen, M. Gradzielski, A. Laschewsky and D. Neher, *J. Phys. Chem. B*, 2013, **117**, 14576-14587.

22. (a) J. Berger, M. Reist, J. M. Mayer, O. Felt and R. Gurny, *Eur. J. Pharm. Biopharm.*, 2004, **57**, 35-52; (b) J. Berger, M. Reist, J. M. Mayer, O. Felt, N. A. Peppas and R. Gurny, *Eur. J. Pharm. Biopharm.*, 2004, **57**, 19-34.

23. J. Yu, W. Wei, E. Danner, R. K. Ashley, J. N. Israelachvili and J. H. Waite, *Nature Chem. Bio.*, 2011, **7**, 588-590.

TOC Figure:

Ways to orchestrate the mechanical properties and colors of mussel-inspired metal cross-linked hydrogels based on DOPA functionalized cationic polymers are demonstrated. This is achieved by systematically varying the hardness of the coordinating metal and/or the cationic polymer.